JOURNAL OF VIROLOGY, Oct. 1999, p. 8371–8383 Vol. 73, No. 10
0022-538X/99/$04.00+0

The Human Immunodeficiency Virus Type 1 *nef* Gene Can to a Large Extent Replace Simian Immunodeficiency Virus *nef* In Vivo

FRANK KIRCHHOFF,[1]* JAN MÜNCH,[1] SILKE CARL,[1] NICOLE STOLTE,[2] KERSTIN MÄTZ-RENSING,[2] DIETMAR FUCHS,[2] PETER TEN HAAFT,[3] JONATHAN L. HEENEY,[3] TOMEK SWIGUT,[4] JACEK SKOWRONSKI,[4] AND CHRISTIANE STAHL-HENNIG[2]

Institute for Clinical and Molecular Virology, University of Erlangen-Nuernberg, 91054 Erlangen,[1] and German Primate Center, 37077 Göttingen,[2] Germany; Biomedical Primate Research Center, Department of Virology, 2288 GJ Rijswijk, The Netherlands[3]; and Cold Spring Harbor Laboratory, Cold Spring Harbor, New York 11724[4]

Received 29 December 1998/Accepted 12 July 1999

The *nef* gene of the pathogenic simian immunodeficiency virus (SIV) 239 clone was replaced with primary human immunodeficiency virus type 1 (HIV-1) *nef* alleles to investigate whether HIV-1 Nef can substitute for SIV Nef in vivo. Initially, two rhesus macaques were infected with the chimeric viruses (Nef-SHIVs). Most of the *nef* alleles obtained from both animals predicted intact open reading frames. Furthermore, forms containing upstream nucleotide substitutions that enhanced expression of the inserted gene became predominant. One animal maintained high viral loads and slowly progressed to immunodeficiency. *nef* long terminal repeat sequences amplified from this animal were used to generate a second generation of Nef-SHIVs. Two macaques, which were subsequently infected with a mixture of cloned chimeric viruses, showed high viral loads and progressed to fatal immunodeficiency. Five macaques received a single molecular clone, named SHIV-40K6. The SHIV-40K6 *nef* allele was active in CD4 and class I major histocompatibility complex downregulation and enhanced viral infectivity and replication. Notably, all of the macaques inoculated with SHIV-40K6 showed high levels of viral replication early in infection. During later stages, however, the course of infection was variable. Three animals maintained high viral loads and developed immunodeficiency. Of the remaining two macaques, which showed decreasing viral loads after the acute phase of infection, only one efficiently controlled viral replication and remained asymptomatic during 1.5 years of follow-up. The other animal showed an increasing viral load and developed signs of progressive infection during later stages. Our data demonstrate that HIV-1 *nef* can, to a large extent, functionally replace SIVmac *nef* in vivo.

Experimental infection of rhesus macaques with simian immunodeficiency virus (SIV) has demonstrated that an intact *nef* gene is important for maintaining high virus loads and for the development of immunodeficiency (36). The observation that some long-term nonprogressors with human immunodeficiency virus type 1 (HIV-1) infection harbor *nef*-defective viruses (16, 39, 59) suggests a similar importance for the pathogenicity of HIV-1 in humans. SIV Nef and HIV Nef show similar in vitro activities: downmodulation of CD4 and of class I major histocompatibility complex (MHC) cell surface expression (1, 3, 7, 12, 21, 27, 46, 50, 60, 62), enhancement of virion infectivity (22, 43, 52, 69), and stimulation of replication in primary lymphocytes (10, 18, 43, 52, 69). Moreover, both are able to alter T-cell signaling pathways (2, 5, 15, 19, 25, 33, 48, 49, 67) and interact with cellular serine/threonine and tyrosine kinases (11, 19, 32, 44, 45, 54, 58, 61, 66).

Although HIV-1 Nef and SIV Nef perform similar in vitro functions, some noteworthy differences exist. In contrast to HIV-1 *nef*, the SIV *nef* gene overlaps the *env* gene and encodes a protein that has a higher molecular mass (33 to 36 kDa) than HIV-1 Nef (27 to 30 kDa). Sequence homology between the SIVmac and HIV-1 Nef proteins is mainly restricted to the N-terminal myristylation signal and the highly conserved central core region (53). HIV-1 Nef and SIV Nef use overlapping but distinct target sites for CD4 downregulation (31) and may utilize distinct motifs for the interaction with cellular adapter complexes (8, 13, 24, 48, 55). A putative SH3 binding domain $(PxxP)_3$ is highly conserved in HIV-1 Nef and important for the binding of Src family tyrosine kinases Hck and Fyn (4, 44, 58). SIV Nef contains only two prolines at the corresponding position (PxxP) that are dispensable for Src association and of little importance for SIV pathogenicity (37, 43). Recently, it has been shown that SIVmac Nef and HIV-2 Nef, but not HIV-1 Nef, interact with the zeta chain of the T-cell receptor (6, 30). It seems that SIV Nef and HIV-1 Nef are functionally homologous but that several functions involve different interactions.

Investigators have constructed a variety of SIV-HIV chimeric viruses (SHIVs) to address pathogenicity and vaccine issues related to the incorporated HIV-1 gene sequences (63). Recently, molecular SHIV clones that replicate to high levels and induce an AIDS-like disease in macaques have been reported (34, 64). However, all of these pathogenic SHIV constructs carry the SIV *nef* gene and the corresponding clones containing HIV-1 *nef* usually failed to induce high viral loads and immunodeficiency (64). Thus, although functional equivalence between HIV-1 and SIV Nef has been demonstrated in in vitro infectivity and replication systems (66), no animal model suitable for the study of the role of the HIV-1 *nef* gene in viral pathogenicity has been described.

Nef plays an important role in AIDS pathogenesis and may represent a key factor in the development of a live attenuated AIDS vaccine. Nef-SHIVs might allow the elucidation of which

* Corresponding author. Mailing address: Institute for Clinical and Molecular Virology, University of Erlangen-Nuernberg, Schlossgarten 4, 91054 Erlangen, Germany. Phone: 49-9131-852 6483. Fax: 49-9131-852 2101. E-mail: fkkirchh@viro.med.uni-erlangen.de.

in vitro functions of Nef are critical for disease progression in vivo and also provide an animal model for testing of HIV-1 Nef inhibitors. It is unknown whether HIV-1 Nef can substitute for SIV Nef in vivo. Therefore, we have replaced the *nef* gene of the well-characterized pathogenic SIVmac239 clone (35, 36, 57) with a pool of primary HIV-1 *nef* alleles. In the first passage, these chimeras showed little pathogenicity in infected macaques. However, a selective pressure for open functional HIV-1 *nef* open reading frames (ORFs) and for efficient Nef expression could be demonstrated. A second generation of molecularly cloned Nef-SHIVs showed consistently high levels of replication during acute infection and caused immunodeficiency in the majority of infected rhesus macaques. One chronically infected animal, however, efficiently controlled Nef-SHIV replication and remained asymptomatic. It remains to be elucidated if differences in Nef expression levels or in functional aspects are the major reason why Nef-SHIVs seem to induce disease less reproducibly than SIVmac239 *nef*-open.

MATERIALS AND METHODS

Construction of Nef-SHIVs. The pBRΔNU proviral construct was used for the insertion of HIV-1 *nef* genes into the SIV genome (Fig. 1A). This clone contains deletions of 513 bp in the *nef* long terminal repeat (LTR) region and mutations in the SIV *nef* initiation codon and a second ATG at codon 7 of the *nef* ORF (26). These mutations did not alter the predicted Env sequence. Two oligonucleotides (5′-CCGGACCGCGGCCGCCGCTCGCGACGCGT-3′ and 5′-CCG GACGCGTCGCGAGCGGCGGCCGCGGT-3′) were used to insert a 5′-*Not*I-*Nru*I-*Mlu*I-3′ polylinker into the *Xma*I site of pBRΔNU (pBRΔNU-PL). Fragments spanning the *nef* gene were amplified from patient-derived peripheral blood mononuclear cells (PBMC) as described previously (39) and used as templates for amplification with primers pF107 (5′-TTTT**GCGGCCGC**ATGGG TGGCAAGTGGTCA-3′) and pF103 (5′-GCAAGC**ACCGT**TCAGCAGTCTT GTAGTACTCCGGATG-3′) (Fig. 1B). The digested, gel-purified PCR fragments were pooled and cloned into the pBRΔNU-PL vector by using the *Not*I and *Mlu*I sites (in boldface) inserted just upstream of the HIV-1 *nef* initiation codon and downstream of the TGA *nef* termination codon (underlined). Aliquots of transformed supercompetent *Escherichia coli* XL-2 (Stratagene) were plated on Luria broth-ampicillin dishes to assess transformation efficiency, and the remaining 90% of the transformed bacteria were used for direct inoculation of large-scale plasmid preparations. The percentage of the plasmid population containing an HIV-1 *nef* insert was estimated by restriction and PCR analysis (Fig. 2). As a control, the NL4-3 *nef* allele was also inserted into pBRΔNU-PL to generate SHIV-NL43nef.

DNA sequences spanning the 3′ end of the SIV *env* gene, the HIV-1 *nef* gene, and the SIV 3′ LTR were amplified by one round of PCR amplification using primers pNeMu1 (5′-GGAGTAATACTGTTAAGAATAGTG-3′); 8957→8980) and pNeMu2 (5′-CTTCAA**GAATTC**TGCTAGGGATTTTCC-3′) for the construction of the second generation of Nef-SHIVs. Whole cellular DNA isolated from CEMx174 cells, cocultivated with PBMC obtained from Mm7745 at 40 weeks postinfection (wpi), was used as a template. The 1.7-kb hybrid *env-nef*-LTR fragments were sequenced and inserted into a modified pBR322 vector containing the full-length SIVmac239 provirus by using the unique *Nhe*I and *Eco*RI sites (in bold type) in SIV *env* and the vector sequences flanking the 3′ end of the provirus as described previously (43).

Production of virus stocks. COS cells were transfected and virus stocks were generated as described previously (14). 293T cells were transfected by the calcium phosphate method (17) with 10 μg of the proviral constructs. The medium was changed after overnight incubation, and virus was harvested 24 h later. Viral stocks were aliquoted and frozen at −80°C; p27 antigen concentrations of viral stocks were quantitated with a commercial HIV-1–HIV-2 enzyme-linked immunosorbent assay (Immunogenetics, Zwijndrecht, Belgium).

Cells, infectivity, and viral replication. COS, 293T, and sMAGI cells were grown in Dulbecco modified Eagle medium supplemented with 10% fetal calf serum (FCS). Infection of sMAGI cells was performed as described previously (9), and viral infectivity was quantitated by using the Galacto-Light Plus chemiluminescence reporter assay kit (Tropix, Bedford, Mass.) as recommended by the manufacturer. CEMx174 cells were maintained and virus production was measured by reverse transcriptase assay as previously described (56). The herpesvirus saimiri-transformed T-cell line 221 (2) was maintained in the presence of 100 U of interleukin-2 per ml (Boehringer, Heidelberg, Germany) and 20% FCS, and infections were performed in the presence of 50 U of interleukin-2 per ml and 5% FCS. Rhesus PBMC were isolated, cultured, and infected with virus stocks containing 2 ng of p27 as described previously (43). The SIVmac239 *nef** variant, containing a premature in-frame TAA stop signal at the 93rd codon of *nef*, was used as a *nef*-defective control (36).

Infection of rhesus macaques and clinical assessment. Juvenile rhesus macaques of Indian origin were experimentally infected by intravenous inoculation of the Nef-SHIV stocks containing 10 (first experiment) or 5 (second experiment) ng of p27 produced by transfected COS-7 cells. The animals were healthy and seronegative for SIV, type D retrovirus, and simian T-cell lymphotropic virus type 1 at the time of infection. Serological, virological, and immunological analyses were performed as described previously (20, 70–72).

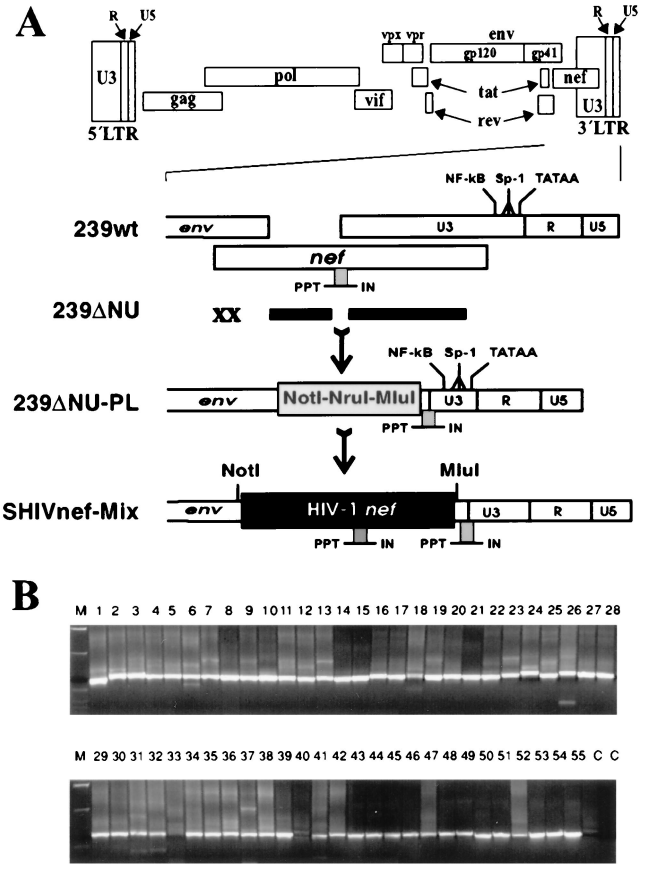

FIG. 1. Generation of chimeric SIVmac239 carrying a complex mixture of primary HIV-1 *nef* alleles. (A) Schematic representation of the SIVmac239 genome (top) and the cloning strategy (below). The original SIVmac239 *nef* initiation codon and a second ATG at amino acid position 7 of the *nef* ORF were mutated, and the *nef* unique region and upstream U3 sequences were deleted to generate 239ΔNU (26). Subsequently, a polylinker was inserted just downstream of the *env* gene (ΔNU-PL) and HIV-1 *nef* genes were cloned into the unique *Not*I and *Mlu*I restriction sites. The deletions in ΔNU are indicated by black bars, and the mutations in the ATGs are indicated by an X; underneath, the positions of the inserted polylinker and the HIV-1 *nef* genes are indicated. PPT, polypurine tract; IN, U3 sequences required for integration. (B) Amplification of HIV-1 *nef* genes from 55 HIV-1-infected individuals with different rates of disease progression. PCR amplification products were digested with *Not*I and *Mlu*I and separated by electrophoresis through 1.5% agarose gels. Cloning into the ΔNU-PL vector was performed as described in Materials and Methods. M, marker; C, negative control. Numbers specify individual patients.

Nef sequence analysis. DNA sequences spanning HIV-1 *nef* were either amplified directly from sequential PBMC DNA samples with a nested PCR approach (38) or obtained from whole cellular DNA isolated from positive PBMC-CEMx174 bulk cocultivation followed by one round of PCR amplification. To detect alterations upstream of the inserted HIV-1 *nef* gene and in the remaining SIV 3′ LTR sequences, fragments spanning the 3′ *env-nef*-LTR region were amplified from virus-positive bulk cocultivations by using primers pNeMu1 and pNeMu2 and cloned and sequenced as described above.

Luciferase expression constructs. The generation of an *env*-deficient SIVmac239 reporter construct (pBR239ΔenvLuc) has been described previously (40). An *Nhe*I-*Bgl*I restriction fragment containing the luciferase gene was used to replace the corresponding region of pBR239 to generate a replication-competent reporter virus. The region between the *Nhe*I site and the inserted luciferase gene was replaced with the corresponding region of the Nef-SHIV-K6 clone by using standard DNA techniques.

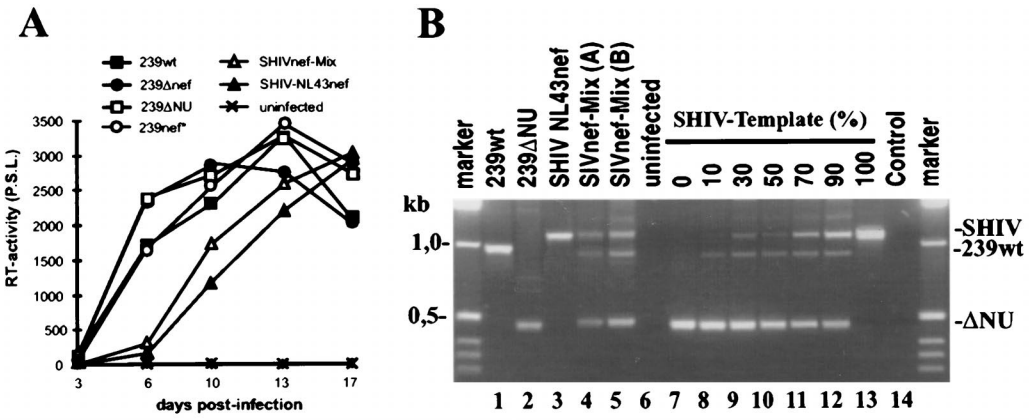

FIG. 2. Characterization of SHIVnef-Mix in vitro. (A) Replication of the indicated SIVmac239 *nef* variants in CEMx174 cells. Cells were infected with virus stocks containing 5 ng of p27 core antigen derived from transfected COS-1 cells. RT, reverse transcriptase; P.S.L., photostimulated light emission. (B) Amplification of the *nef* region from infected (lanes 1 to 4) and uninfected (lane 6) CEMx174 cells. Genomic DNA was extracted at 10 days postinfection. For comparison, 0.2 ng of the pBR-SHIVnef-Mix plasmid preparation was used as the template for amplification (lane 5). To assess relative amplification efficiencies, the ΔNU and SHIV templates were mixed at different molar ratios (lanes 7 to 13). The expected positions of fragments representing 239nef, the ΔNU mutant, and the chimeras are indicated. Control, no DNA added to the PCR mixture.

Functional analysis. Dose-response analysis of the effect of Nef on CD4 and MHC class I cell surface expression was performed as described previously (24, 50, 68). The effect of Nef expression on CD3-initiated signaling, as revealed by CD69 induction in response to an anti-CD3 monoclonal antibody (MAb), was assayed as previously described (33). Briefly, Jurkat T cells were electroporated with 25 μg of DNA containing 3 μg of cytomegalovirus CD20 marker plasmid and various amounts of expression plasmids and carrier DNA. At 18 to 24 h after transfection, cells were stimulated by overnight incubation with anti-CD3 MAb HIT3A (PharMingen). To reveal CD4 and MHC class I surface expression, cells were incubated for 1 h on ice with PerCP-conjugated anti-CD20 MAb Leu-16 (Becton Dickinson) for 30 to 36 h after transfection and phycoerythrin-conjugated anti-CD4 MAb Leu3A (Becton Dickinson) together with fluorescein isothiocyanate-conjugated anti-HLA A, B, and C MAb G46-2.6 (PharMingen). To reveal CD69 expression, cells were incubated with fluorescein isothiocyanate-conjugated anti-CD69 MAb FN50 (PharMingen). CD4, CD20, CD69, and class I MHC surface expression was analyzed by using an Epics-Elite flow cytometer. For dose-response analysis, CD4, CD69, or class I MHC levels are represented by the peak channel number of red or green fluorescence on $CD20^+$ cells.

Western blot analysis. CEMx174 cells were infected with virus containing 10 ng of p27 core antigen derived from transfected 293T cells. When cytopathic effects were observed, cells were harvested and expression of Nef proteins in whole cellular lysates was analyzed by immunoblotting using rabbit anti-Nef serum (19). For detection of p27 core protein, an anti-Gag serum derived from SIVmac p27 hybridoma cells (55-2F12) was used (28). For enhanced chemiluminescence detection, horseradish peroxidase-conjugated secondary antibodies were used as described by the manufacturer of the ECL detection system (Amersham, Chicago, Ill.).

RESULTS

Construction of SHIVs containing primary HIV-1 *nef* alleles. Our strategy to obtain pathogenic Nef-SHIVs was to maximize the genetic information in the proviral constructs used in the initial study and to utilize the selective pressure in vivo as a tool to select for those forms that replicate and persist most efficiently in infected macaques. Therefore, the SIVmac *nef* gene was replaced with a complex mixture of primary HIV-1 *nef* alleles amplified from 55 HIV-1-infected individuals (Fig. 1B). Furthermore, the proviral constructs contained two regions encompassing the polypurine tract and the U3 sequences required for integration. One is located in the inserted HIV-1 *nef* gene, and a second is just upstream of the SIV core enhancer elements (Fig. 1A). Based on previous observations (38), we expected that sequences not advantageous for viral replication would be efficiently deleted or mutated in vivo.

As described in Materials and Methods, the HIV-1 *nef* PCR fragments were cloned as a pool into the pBRΔNU-PL construct. Control experiments indicated that the plasmid preparation (named pBR-SHIVnef-Mix) represented approximately 80,000 transformants and that about 90% of the plasmid population contained an insert of the expected size (data not shown). Ten colonies were randomly picked and analyzed. Nine clones contained an HIV-1 *nef* gene, and one represented the original pBRΔNU-PL construct. The *nef* sequences were heterogeneous and likely all originated from different HIV-1-infected individuals (data not shown).

Virus stocks were generated by transient transfection of COS-1 cells with the pBR-SHIVnef-Mix DNA preparation and used for infection of CEMx174 cells. The virus population was replication competent. However, similar to infection with SHIV-NL43nef, the replication kinetics were slightly delayed compared to those of the *nef*-open and *nef*-defective SIVmac239 controls (Fig. 2A). Both the chimeric proviral sequences and those with *nef* deleted were readily detectable in infected CEMx174 cells (Fig. 2B, lane 4). PCR analysis of the plasmid population used for transient COS-1 transfection yielded a similar pattern (Fig. 2B, lane 5). The shorter ΔNU template was amplified more efficiently than the SHIV template (Fig. 2B, lanes 7 to 13). Thus, the results of the PCR analysis are in agreement with the restriction analysis and indicate that the majority of the plasmid population used for transfection and most of the proviral sequences in infected cells contained an inserted HIV-1 *nef* gene.

Low pathogenicity of the first generation of Nef-SHIVs. Two juvenile rhesus macaques, Mm7739 and Mm7745, were infected intravenously with aliquots of the virus stocks obtained after transient transfection of COS-1 cells with pBR-SHIVnef-Mix. The viral inoculum contained 10 ng of p27 antigen, which corresponded to approximately 10,000 50% tissue culture-infective doses for CEMx174 cells. Unexpectedly, very early after infection, predominantly the 239-ΔNU-PL virus with *nef* deleted could be detected (Fig. 3A). However, in both animals, the chimeras came to predominate by 2 to 4 wpi, indicating a selective pressure for HIV-1 *nef*-containing forms. The p27 antigen levels during the acute phase of infection were low, compared to those measured after wild-type 239 (239wt) infection (Table 1). Both animals developed strong humoral immune responses. Only Mm7745 showed persistently high cell-associated viral loads (Fig. 3B). The $CD4^+$ T-cell numbers were stable in Mm7739 and decreased only slightly in Mm7745

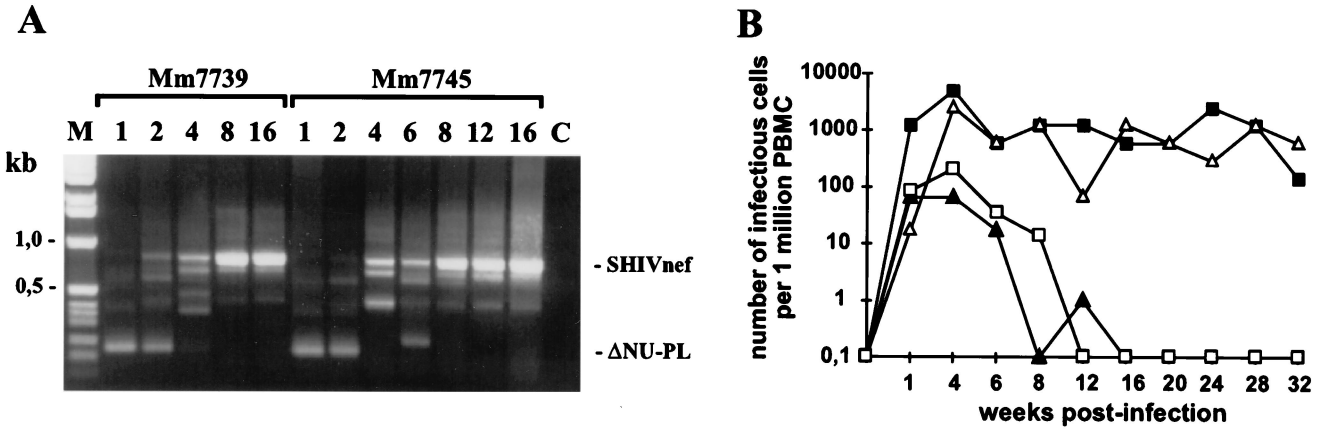

FIG. 3. In vivo properties of SHIVnef-Mix. (A) Nef-LTR sequences were amplified from positive PBMC-CEMx174 bulk cocultivations, obtained at the indicated times (weeks postinfection), and separated on a 1.5% agarose gel. Similar results were obtained by nested PCR using DNA extracted from PBMC. M, marker, C, control. (B) Cell-associated viral load. The values shown are for Mm7739 (▲) and Mm7745 (△) inoculated with the SHIVnef-Mix stock, one 239wt-infected animal (■), and averages obtained from four macaques infected with ΔNU (□) (26).

(data not shown). Mm7739 developed mild (12 wpi)-to-moderate (40 wpi) lymphadenopathy and remained clinically healthy with low viral loads throughout the 74-wpi observation period. Mm7745 lost body weight and had to be euthanized at 84 wpi because of weakness. Postmortem examination revealed severe hyperplasia to depletion of the germinal centers of the lymph nodes, severe multiorgan vasculitis and perivasculitis with evidence of cytomegalovirus infection, and moderate activation of microglia cells. Both animals were infected with the same virus stock. Therefore, it was unexpected that the cell-associated virus load was similar to *nef*-deleted infection of Mm7739 but comparable to SIVmac239 *nef*-open infection of Mm7745 (Fig. 3B).

Selective pressure for intact HIV-1 *nef* genes and for upstream nucleotide substitutions. We sequenced PCR fragments spanning the inserted HIV-1 *nef* genes derived from PBMC samples and from reisolation bulk cultures to investigate whether (i) the HIV-1 *nef* genes remained intact, (ii) specific *nef* variants came to predominate, or (iii) consistent sequence alterations occurred upstream or downstream of the inserted *nef* genes. Nine of 10 *nef*-spanning fragments amplified from PBMC obtained from Mm7739 at 12 wpi and 25 of 27 clones obtained from the spleen, lymph nodes, or thymus at 74 wpi predicted an intact *nef* ORF (Fig. 4 and data not shown). Similarly, 37 (95%) of 39 *nef* ORFs amplified from the progressing animal, Mm7745, at different time points were intact. These frequencies of intact *nef* alleles are similar to those observed in human HIV-1 infection (32, 65) and indicate a strong selective pressure for open functional HIV-1 *nef* genes, even in the animal with the low viral load.

Several previously defined conserved motifs in HIV-1 Nef (41, 65) were also conserved in the deduced Nef sequences obtained from the infected macaques: an N-terminal myristylation signal, a PxxP motif, a putative protein kinase C recognition site, a predicted β-turn, and a dileucine motif (13) (Fig. 4). However, some unusual amino acid variations, that are rarely present in HIV-1 Nef sequences derived from infected humans (32, 41, 51, 65), are notable. These include alterations close to the N terminus of Nef (G3A, K4R, and W5L), mutation of a usually highly conserved cysteine (C55V), and the presence of a glycine residue in the central part of the acidic region (EEGEE) (Fig. 4 and data not shown). For most of these variations, it is unclear if they were already present in the initial *nef* pool or occurred during in vivo selection. However, the oligonucleotide used for amplification of the HIV-1 *nef* genes predicted the N-terminal sequence MGGKWS. All 25 *nef* alleles amplified from both macaques at 12 wpi also predicted MGGKWS, whereas 25 (86%) of 29 deduced Nef amino acid sequences obtained at later time points contained alterations in this region. Therefore, it seems likely that the changes close to the N terminus emerged during the course of infection. The K4R, C55V, and EEGEE changes were not present in all of the clones obtained at late time points from the progressing animal and were also detected in the asymptomatic animal, Mm7739 (Fig. 4). Thus, these sequence variations are not linked to disease progression. Nonetheless, since they were frequently observed in both animals, these HIV-1 Nef features may be advantageous for SIV replication in macaques.

To generate Nef-SHIVs with enhanced pathogenicity and to investigate which upstream and downstream changes are selected, 1.7-kb fragments spanning the 500 bp upstream of *nef* and the entire 3′ LTR were amplified from positive bulk cocultures obtained from the progressing animal, Mm7745, at 40 wpi. Sequence analysis revealed the following consistent changes upstream of the inserted *nef* gene: A9110G (15 of 15, predicting amino acid changes of Env R751G and Rev K41R), A9224G (12 of 15, predicting Env T789A and Rev N79C), T9276C (4 of 15, predicting Rev C97R), G9277C (9 of 15, predicting Env A807P and Rev C97S), A9442G (12 of 15), and T9276C (3 of 15, predicting Rev C97R) (Fig. 5). Numbering refers to the SIVmac239 sequence (57). Furthermore, a change of C→A was observed at the *Not*I site. Most of these upstream changes were already present in the majority of clones obtained from Mm7745, but not in those from Mm7739, at 12 wpi (data not shown). However, at the 74-week necropsy time point, changes at nucleotide positions 9276 or 9277 and 9442 and the C→A change at the *Not*I site were also detected in all 27 of the *nef*-LTR fragments amplified from lymphatic tissues obtained from the asymptomatic animal, Mm7739.

Changes downstream of the HIV-1 *nef* genes were rarely observed. Three of the 15 clones obtained from Mm7745 at 40 wpi contained a deletion of 36 bp removing the SIV polypurine tract and the SIV U3 sequences required for integration (Fig. 5). This deletion was detected in fragments carrying highly divergent *nef* alleles (7745-40wk1, 7745-40wk8, and 7745-40wk10; Fig. 4). Thus, it seems likely that the deletion evolved

TABLE 1. Viral load and nonspecific immune activation in macaques infected with Nef-SHIVs

Animal(s)[a]	Virus used for infection	Acute phase (first 6 wpi)[b]				Postacute phase (after 12 wpi)[c]			
		p27 concn (pg/ml)	Viral load	Neopterin	RNA[d]	p27 concn (pg/ml)	Viral load	Neopterin	RNA[d]
Mm7739	SHIVnef-Mix	56	66	4.9	ND[e]	BQL[f]	0–0.1	1.0	ND
Mm7745	SHIVnef-Mix	287	2,500	4.2	ND	BQL	285–1,250	3.9	ND
Mm8655	SHIV-40Mix	5,482	2,048	8.8	1.9×10^7	37	256–4,096	3.6	1.1×10^7
Mm8664	SHIV-40Mix	756	4,096	11.1	8.9×10^6	16,000	1,024–8,192	8.1	6.4×10^6
Mm8653	SHIV-40K6	795	4,096	3.4	4.6×10^6	86	0.0–8	1.8	1.7×10^3
Mm8658	SHIV-40K6	3,562	4,096	6.3	2.6×10^7	337	32–1,024	6.6	1.4×10^7
Mm7746	SHIV-40K6	384	1,028	7.0	9.4×10^5	BQL	2–32	4.7	2.0×10^5
Mm7793	SHIV-40K6	2,952	8,192	12.3	1.0×10^7	BQL	128–2,048	7.0	2.9×10^6
Mm8014	SHIV-40K6	1,208	4,096	8.4	1.0×10^7	579	256–4,096	9.8	8.5×10^6
Mm ($n = 5$)	SHIV-40K6	1,780 ± 1,249	4,302 ± 2,279	7.5 ± 2.9	$1.0 \times 10^7 \pm 8.6 \times 10^6$	3+/2 BQL	0.0–4,096	1.8–9.8	$5.1 \times 10^6 \pm 5.4 \times 10^6$
Mm ($n = 9$)	239wt	4,311 ± 3,049	2,786 ± 1,556	10.5 ± 3.1	$1.1 \times 10^7 \pm 7.5 \times 10^6$	3+/6 BQL	128–4,096	1.5–10.3	$1.6 \times 10^6 \pm 1.4 \times 10^6$
Mm ($n = 4$)	ΔNU	67 ± 39	590	2.8 ± 1.1	$1.8 \times 10^5 \pm 1.2 \times 10^5$	BQL	0.0–0.3	0.6–1.4	$3.9 \times 10^3 \pm 8.3 \times 10^3$

[a] Animals were housed at the German Primate Center. Mm, *Macaca mulatta*.
[b] The highest value observed during the first 6 weeks after infection is shown. Viral load is given as the number of infected cells per million PBMC. The neopterin level is given as fold of baseline. The RNA level is the number of copies per milliliter of plasma. For the viral load of the ΔNU-infected macaques, the end point was not reached at 2 wpi.
[c] Surviving animals were observed at least until 52 wpi. Peak values are given for p27, neopterin, and RNA load; ranges are given for the cell-associated viral load.
[d] RNA values for SIV *nef*-open and *nef*-defective controls were derived from 10 ΔNU-infected and 7 SIVmac32H/1XC-infected rhesus macaques housed at the Biomedical Primate Research Center in Rijswijk, The Netherlands (72).
[e] ND, not determined.
[f] BQL, below quantitation limit.

independently in the progressing animal and that the intact SIV polypurine tract and U3 sequences required for integration are not important for replication of Nef-SHIVs in macaques. No changes in the mutated SIV *nef* ATGs, the HIV-1 polypurine tract, or the HIV-1 U3 sequences required for integration were detected.

The upstream changes enhance gene expression. Some of the nucleotide substitutions observed upstream of the inserted HIV-1 *nef* genes were likely to influence protein expression. For example, the change at position 9442 or 9443 removed an upstream ATG that is not in frame with the original SIV *nef* ORF or the inserted HIV-1 *nef* gene. The C-to-A change at the *Not*I site generates higher homology to the optimal translation initiation sequence (42).

To test the influence of these changes on viral infectivity and gene expression, the luciferase gene was inserted between the *Not*I and *Mlu*I restriction sites in the pBR239ΔNU-PL construct to obtain a replication-competent reporter virus (239ΔNU-Luc). The region upstream of the inserted luciferase (*Nhe*I to *Sst*II) gene was subsequently replaced with the corresponding region of the Nef-SHIV-K6 clone to generate 239-K6NS-Luc (Fig. 5). Compared to SIVmac239, this fragment contains mutations of A9110G, A9224G, T9276C, and A9442G. The C-to-A change selected at the *Not*I site, located just upstream of the inserted *nef* genes, is not present in this construct. sMAGI and CEMx174-SEAP reporter cell lines were infected, and the expression of the cell-associated reporter genes and that of the viral luciferase gene were measured in parallel to assess the influence of the upstream changes selected in vivo on both infectivity and expression of the inserted gene. The β-galactosidase (sMAGI) and secreted alkaline phosphatase (CEMx174) activities were only slightly higher after infection with the 239-K6NS-Luc variant than after infection with 239ΔNU-Luc (Fig. 6). The luciferase activities, however, were consistently approximately threefold higher for the virus containing the upstream changes selected in Mm7745 (Fig. 6). This result suggests that selective pressure for efficient expression of the inserted HIV-1 *nef* gene in vivo exists. The C-to-A change at the *Not*I site is likely to further enhance gene expression. In agreement with this assumption, we detected larger amounts of Nef protein in CEMx174 cells infected with Nef-SHIV-40K6 than in cells infected with SHIV-NL43nef (data not shown).

HIV-1 *nef* alleles derived from Mm7745 are functionally active. Six *env-nef*-LTR fragments derived from Mm7745 at 40 wpi were inserted into the pBR239wt vector by using the single *Nhe*I and *Eco*RI sites (Fig. 5) and used to produce virus stocks by transient transfection of 293T cells. All six Nef-SHIVs showed reduced infectivity in sMAGI cells compared to 239wt (Fig. 7A). However, the infectivity was also reduced when HIV-1 *nef* was replaced with the 239wt *nef* allele (239K6wt) (Fig. 7A). This virus, containing a duplication of 167 bp of the *nef-env* overlapping region, showed lower steady-state levels of Nef expression than SIVmac239wt (Fig. 7B and data not shown). It was more infectious in sMAGI cells, however, than an otherwise isogenic form containing a stop signal at the 93rd codon in *nef* (239K6nef*) (Fig. 7A). Furthermore, a frameshift mutation in the HIV-1 *nef* gene of SHIV-40K6 (K6fr) or mutation of the ATG initiation codon in SHIV-40K13 (K13x) reduced viral infectivity about fourfold (Fig. 7A). Thus, intact HIV-1 *nef* genes were able to enhance SIV infectivity.

The Nef-SHIVs grew with delayed kinetics in CEMx174 cells, in which we never observed a significant difference between nef^+ and nef^- variants of SIVmac239 (an example is shown in Fig. 7C, left). However, the chimeras replicated more efficiently than *nef*-defective SIVmac239 in the herpesvirus

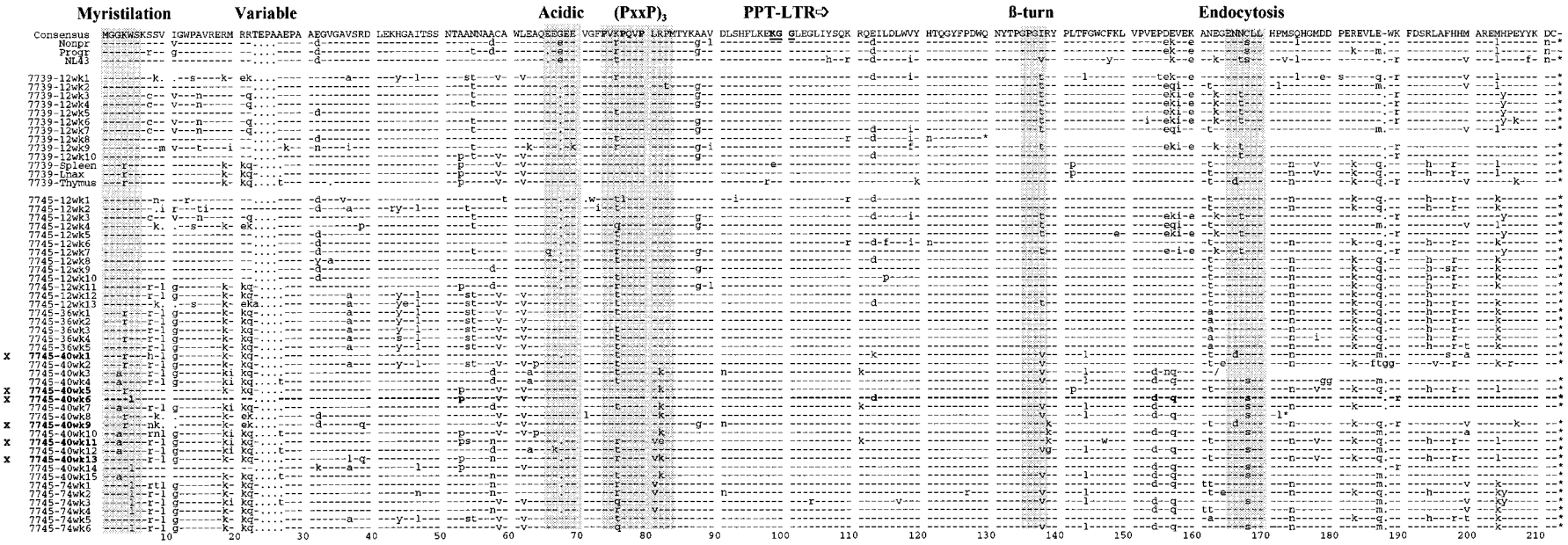

FIG. 4. Alignment of the predicted HIV-1 Nef sequences derived from macaques infected with SHIVnef-Mix. In the left column, the four-digit numbers specify the animals, the two-digit numbers are weeks postinfection, and the last numbers specify the individual clones. *nef*-spanning fragments were amplified from PBMC or from bulk cocultivations obtained at the time points indicated. The Nef sequences derived from the spleen, thymus, and axillary lymph nodes of Mm7739 represent consensus sequences obtained from the analysis of nine cloned *nef* fragments for each tissue. For each time point or tissue, sequences were obtained from at least three independent PCRs. For comparison, HIV-1 Nef consensus sequences derived from 41 nonprogressors (Nonpr) and 50 progressing HIV-1-infected individuals (Progr) are shown. Dashes indicate identity with the consensus Nef sequence, periods indicate gaps introduced to optimize the alignment, and asterisks indicate stop signals. /, frameshift mutation; X, *nef* alleles selected for functional analysis. The SHIV-40K6 sequence is in boldface letters. Some conserved sequence motifs in Nef are indicated by shading.

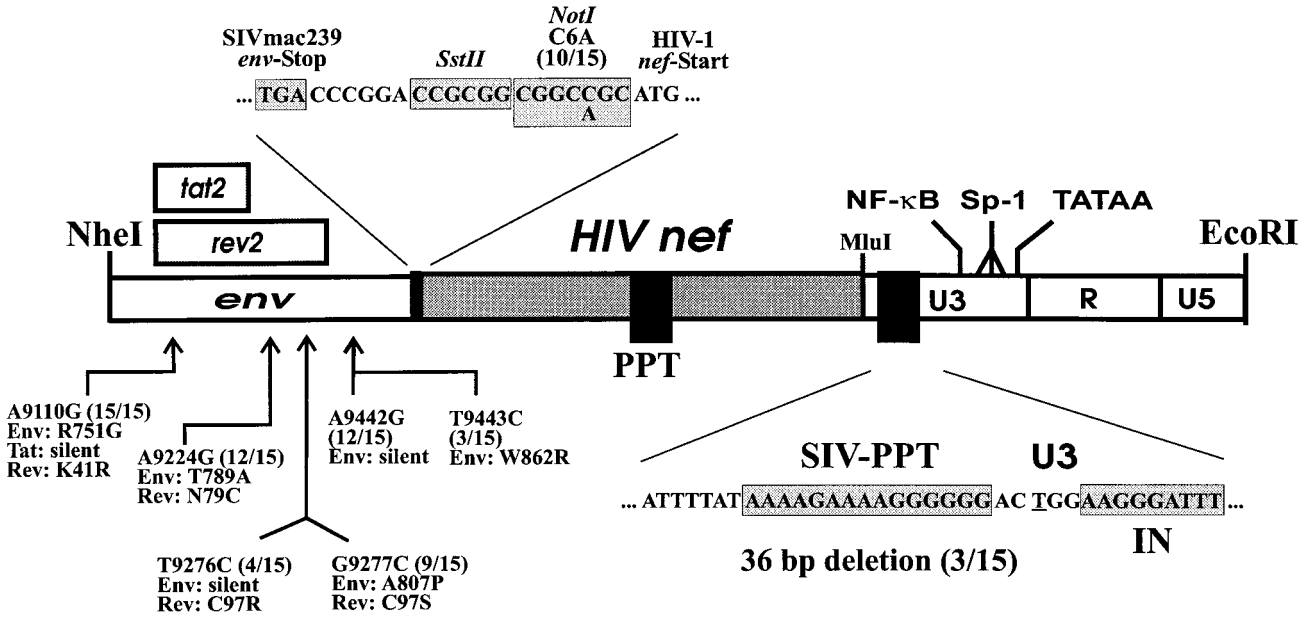

FIG. 5. Nucleotide substitutions and deletions upstream and downstream of the HIV-1 *nef* genes. The positions of changes observed in 15 clones derived from Mm7745 at 40 wpi compared to the pBR-ΔNU-PL construct are indicated; numbering refers to the SIVmac239 sequence (57). Numbers in parentheses indicate the proportion of clones containing the alteration. The corresponding amino acid changes are in the single-letter code. Only alterations observed in at least 3 of the 15 clones are indicated. Abbreviations are defined in the legend to Fig. 1.

saimiri-transformed 221 cell line (Fig. 7C, middle) and in rhesus PBMC (Fig. 7C, right). In contrast, variants of SHIV-40K6 and SHIV-40K13 lacking the initiation codon or containing a frameshift mutation were unable to stimulate viral replication (data not shown).

Five of these HIV-1 *nef* alleles were also tested for the ability to alter T-cell receptor signaling pathways and to downmodulate class I MHC and CD4 cell surface expression. Expression of the 40K1, 40K6, and 40K11 *nef* alleles derived from Mm7745 blocked the induction of CD69 cell surface expression after stimulation with the anti-CD3 MAb (Fig. 8A). Furthermore, transient transfection of Jurkat cells with these *nef* expression constructs resulted in a dose-dependent decrease in surface class I MHC (Fig. 8B) and CD4 (Fig. 8C) expression. The *nef* alleles derived from Mm7745 were almost as active as the strong control HIV-1 NA7 *nef* allele. The remaining two *nef* alleles, 40K5 and 40K13, were nonfunctional in these in vitro assays. Relatively high frequencies of functionally defective *nef* alleles that predict intact ORFs have also been described for human HIV-1 infection (51).

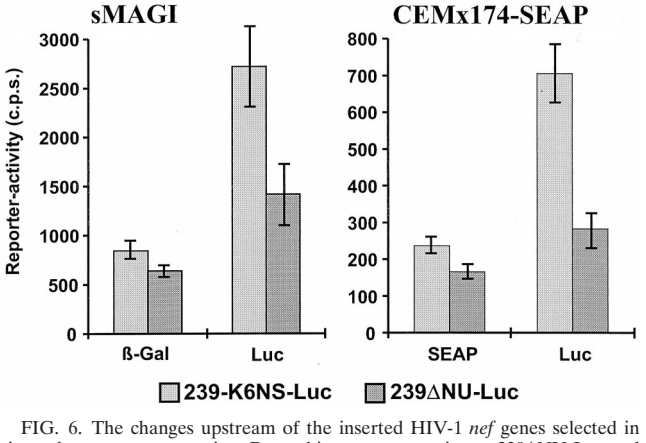

FIG. 6. The changes upstream of the inserted HIV-1 *nef* genes selected in vivo enhance gene expression. Recombinant reporter viruses 239ΔNU-Luc and 239-K6NS-Luc were generated, and expression of the cellular and viral reporter genes was measured as described in Materials and Methods. Infections were performed with virus stocks containing 100 (sMAGI) or 10 (CEMx174-SEAP) ng of p27 antigen. Given are average values obtained from 12 infections performed with four independent virus stocks. c.p.s., counts per second; β-Gal, β-galactosidase; Luc, luciferase; SEAP, secreted alkaline phosphatase.

Pathogenic potential of the second generation of Nef-SHIVs. The progressive status of Mm7745 and the in vitro analysis of the *env-nef*-LTR fragments derived from this animal suggested that the changes selected in vivo might enhance the pathogenicity of the chimeric viruses. To assess the pathogenic potential, two rhesus macaques were infected intravenously with a mixture of cloned Nef-SHIVs, representing the six HIV-1 *nef* alleles indicated in Fig. 4, and five animals were infected with the SHIV-40K6 clone.

Mm8655 and Mm8664, infected with the mixture, showed high viral loads and progressed to fatal immunodeficiency. The characteristics of infection were highly similar to those of infection with pathogenic *nef*-open SIVmac239, i.e., high levels of plasma viremia and viral RNA, persistently high cell-associated viral loads, declining $CD4^+$ cell counts, and about 10-fold elevated levels of neopterin during the acute phase of infection (Fig. 9, Table 1, and data not shown). Both animals were euthanized at 39 (Mm8655) and 40 (Mm8664) weeks after infection, respectively. At the time of death, Mm8655 showed lymph node alterations ranging from severe hyperplasia to depletion of germinal centers and a malignant centroblastic-monomorphic B-cell lymphoma. During the course of infection, this animal showed declining T4/T8 cell ratios and weight loss. Mm8664 developed anemia, thrombocytopenia, and opportunistic *Campylobacter*, *Giardia*, and *Trichomonas* infections. Postmortem examination revealed a generalized follicular hyperplasia together with follicular depletion, *Pneumocystis carinii* pneumonia, and chronic enteritis with bacterial

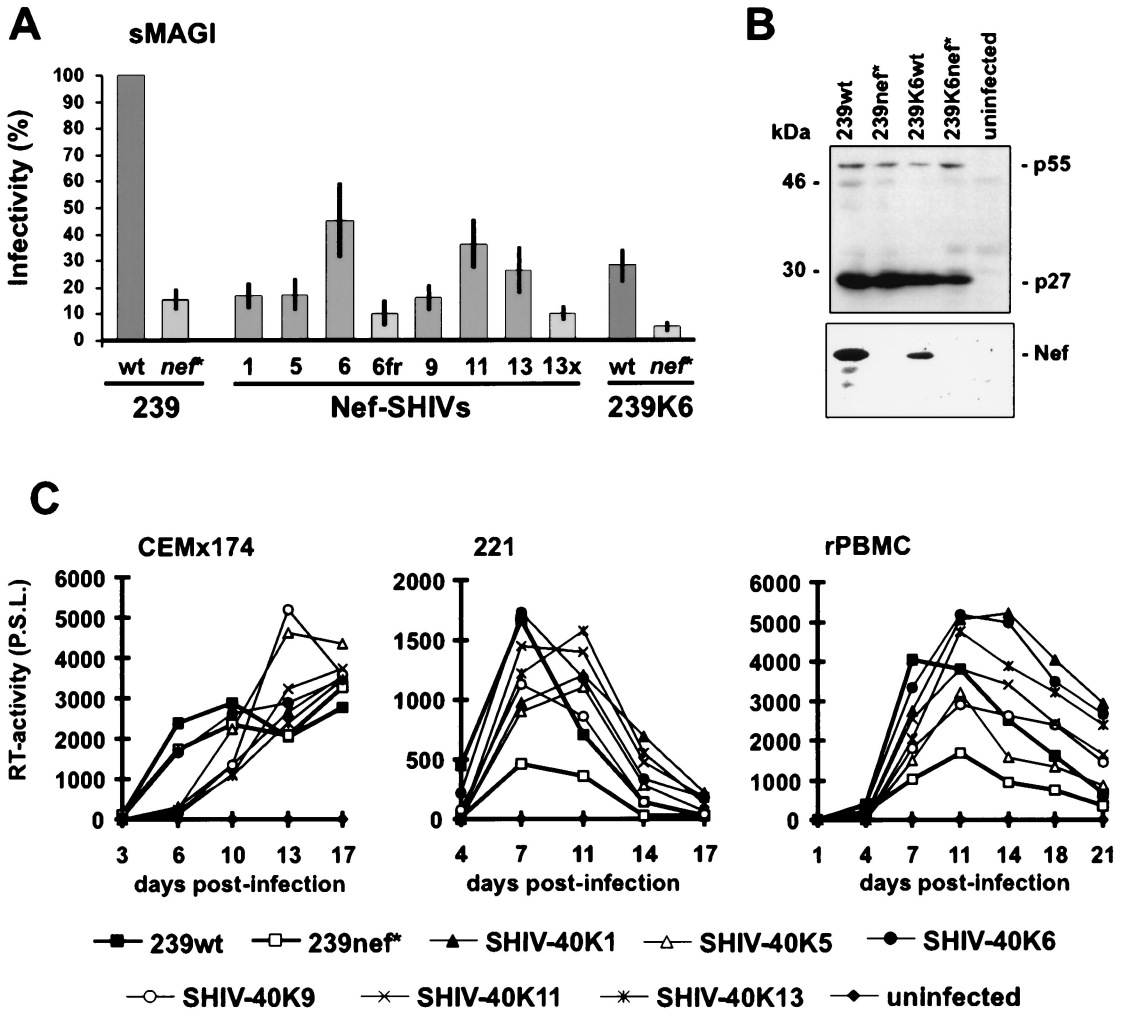

FIG. 7. Infectivity and replication of Nef-SHIVs. (A) sMAGI cells were infected in triplicate with three different virus stocks. The HIV-1 *nef* alleles were derived from Mm7745 at 40 wpi (Fig. 4). As an additional control, a frameshift mutation was inserted at position 23 of the SHIV-40K6 *nef* gene (6fr) and the ATG *nef* initiation codon was mutated in SHIV-40K13 (13×) by overlap extension PCR (29). As shown on the right, HIV-1 *nef* in SHIV-40K6 was replaced with the SIVmac239wt and *nef** genes. Infectivity is shown relative to that of SIVmac239 *nef*-open. Error bars indicate standard deviations. wt, wild type. (B) Detection of the p27 capsid antigen and Nef in CEMx174 cells infected with the mutants indicated. Immunoblotted proteins were detected with anti-Gag serum derived from SIVmac p27 hybridoma cells (55-2F12) (28) or rabbit anti-Nef serum (19). (C) Comparison of the replication kinetics in CEMx174 cells (left), 221 cells (middle), and rhesus PBMC (right). Cells were infected and cultivated as described in Materials and Methods. Similar results were obtained in two independent experiments. RT, reverse transcriptase, P.S.L., photostimulated light emission.

overgrowth. Sequence analysis from PBMC samples revealed that the SHIV-40K11 clone was the predominant form in Mm8655 (8 wpi, four of six clones analyzed; 16 wpi, four of five clones analyzed; and 28 wpi, three of four clones analyzed), although the SHIV-40K6 clone was also detected (8 wpi, two of six clones analyzed; 16 wpi, one of five clones analyzed; and 28 wpi, one of four clones analyzed). The SHIV-40K6 clone predominated in Mm8664 (8 wpi, five of five clones analyzed; 16 wpi, four of five clones analyzed; and 28 wpi, three of three clones analyzed).

Five macaques were inoculated with the molecular SHIV-40K6 clone. This clone was selected because (i) the deduced Nef amino acid sequence showed 94% homology and 90% identity to the HIV-1 consensus Nef sequence, (ii) this chimera showed a phenotype similar to that of the 239 *nef*-open virus in in vitro replication assays (Fig. 7), (iii) the 40K6 *nef* allele was active in cell-based functional assays (Fig. 8), and (iv) this allele came to predominate in the progressing animal Mn8664. All five macaques became infected and developed a humoral immune response against SIV (Fig. 10A). Peak levels of p27 plasma viremia were observed at 2 wpi and ranged from 384 to 3,562 pg/ml (Fig. 10B; Table 1). On average, the detectable p27 levels were 2.5-fold reduced compared to those produced by 239wt infection but 25-fold higher than those compared by infection with SIVmac239 with *nef* deleted and also 10-fold higher than those in the two macaques infected in the initial study (Table 1). Both the viral RNA copy numbers and the cell-associated viral load were similar to those caused by 239 *nef*-open infection during the acute phase of infection (Fig. 10C and D; Table 1). With a single exception (Mm8653), the levels of neopterin, which is a marker for nonspecific immune activation, were also comparable to those observed after infection with pathogenic SIVmac239 (Table 1; Fig. 10F). Thus, during the early phase of infection, the molecular SHIV-40K6 clone replicated about as efficiently in vivo as the parental 239 clone containing SIV *nef*. Thereafter, however, the course of

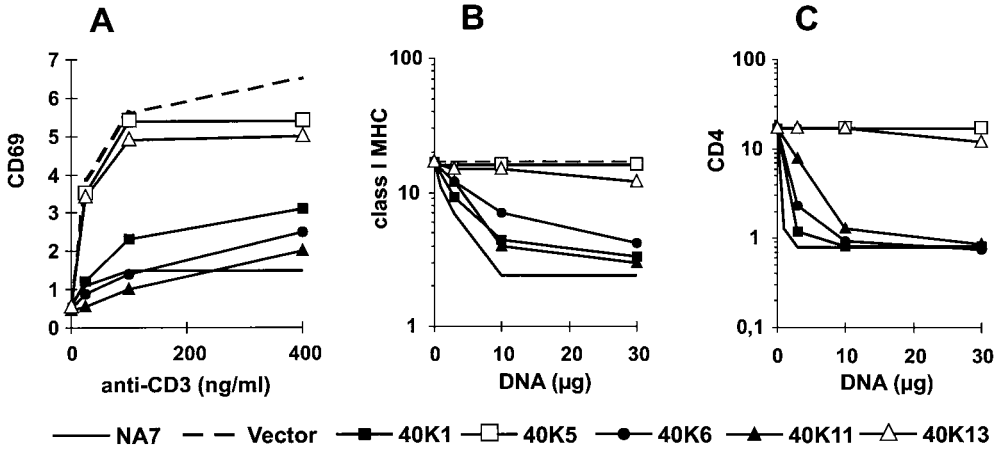

FIG. 8. Functional activity of *nef* alleles derived from Mm7745. (A) Jurkat cells were transfected with the Nef expression constructs and stimulated with the indicated amounts of anti-CD3 MAb to assess the effect of Nef on T-cell receptor signaling. (B) MHC class I downregulation by *nef* alleles derived from Mm7745. (C) *nef* alleles derived from Mm7745 downregulate CD4. Human $CD4^+$ Jurkat T cells were transiently transfected with the indicated amounts of plasmids, and analysis was performed as described in Materials and Methods.

infection differed between individual animals. Three of these five animals, Mm8658, Mm7993, and Mm8014, maintained high virus loads (Fig. 10C and D) and showed declining $CD4^+$ T-cell counts (Fig. 10E). Interestingly, in Mm8658, the number of $CD4^+$ cells increased from 385/mm^3 at 20 wpi to 1,317/mm^3 at 32 wpi (Fig. 10D). Following partial recovery, however, the number of $CD4^+$ lymphocytes started to decrease again after 40 wpi (Fig. 10E). Mm8658 was alive at 80 wpi but maintained a high viral load and a low $CD4^+$ lymphocyte count. This animal developed moderate lymphadenopathy by 8 wpi and severe splenomegaly by 28 wpi. Mm7793 and Mm8014 were also alive at 52 wpi, but both showed persistently high viral loads and developed severe lymphadenopathy, splenomegaly, and thrombocytopenia. In contrast, the RNA copy numbers and cell-associated viral loads strongly decreased after the acute phase of infection in the remaining two animals, Mm8653 and Mm7746 (Fig. 10C and D). Both animals remained clinically healthy and maintained $CD4^+$ lymphocyte counts of >500/mm^3 (Fig. 10E) after 80 (Mm8653) and 52 (Mm7746) weeks of follow-up, respectively. However, efficient control of SHIV-40K6 replication was only temporary in Mm7746 and the viral RNA load increased again by almost 2 logs from 12 to 44 wpi (Fig. 10C). The increase in viral load coincided with progressive lymphadenopathy. Similarly to the three macaques which maintained high viral loads throughout the course of infection, Mm7746 shows increasing neopterin levels, indicating immune activation and progressive infection (Fig. 10F). Of the five animals infected with SHIV-40K6, Mm8653 and Mm7746 showed the lowest levels of replication (assessed by plasma viremia and RNA load) during the acute phase of infection (Table 1). The SIV-specific antibody titers in the progressors were usually higher (204,800 to 819,200) than those observed in the two asymptomatic macaques (51,200 and 204,800), indicating that the humoral immune response did not play a major role in the control of viral replication (Fig. 10A). Nef-LTR sequences were analyzed at 16 wpi (Mm7793, Mm7746, and Mm8014) and 24 wpi (Mm8653 and Mm8658) to investigate if changes in the 3′ *env-nef*-LTR region contributed to the different rates of disease. Compared to the original 40K6 Nef sequence, the alterations were as follows: Mm7793, E28K and P53S; Mm8014, none; Mm8658, I11S, R17K, K32E, N55S, K76R, P80S, and Q130H; Mm8653, K32E, A57D, and P77S; Mm7746, E67K. Unexpectedly, mutations in an otherwise highly conserved $P(xxP)_3$ motif (boldface) were present in *nef* alleles derived from Mm8653 (Pxx**S**xxPxxP) and Mm8658 (Pxx-Pxx**S**xxP). For both animals, the P→S changes were predicted by all six of the *nef* alleles derived from two different PCRs. These alterations were not detected in clones obtained at 6 wpi (data not shown). Compared to SHIV-40K6, no consistent changes in the HIV-1 *nef* flanking regions were detected.

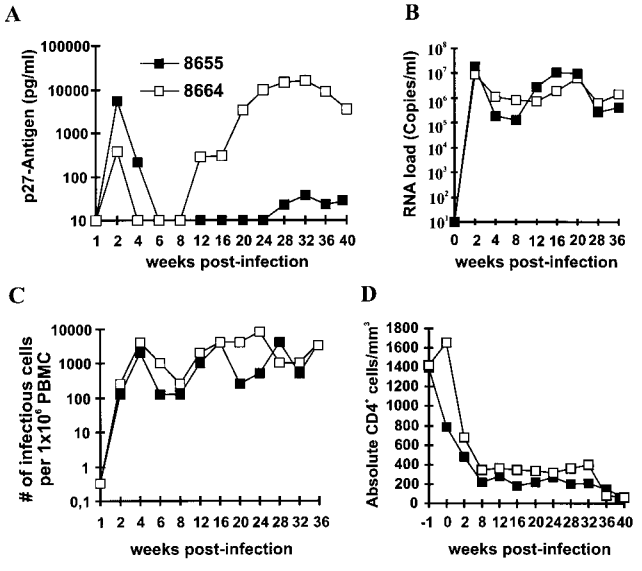

FIG. 9. Replication of SHIV-40mix in rhesus macaques. Two rhesus macaques, Mm8655 and Mm8664, were infected by intravenous inoculation of medium containing a mixture of six different Nef-SHIV clones (Fig. 4). Panels: A, levels of plasma viremia; B, viral RNA load; C, number of infectious cells per million PBMC; D, absolute $CD4^+$ T-cell count. The limit of viral RNA detection is approximately 40 copies/ml (72) of plasma, and for plasma p27 antigen it is about 10 pg/ml of plasma. Values were determined as described in Materials and Methods.

DISCUSSION

In this study, we found that SIV containing the HIV-1 *nef* gene shows efficient replication and can induce $CD4^+$ T-cell

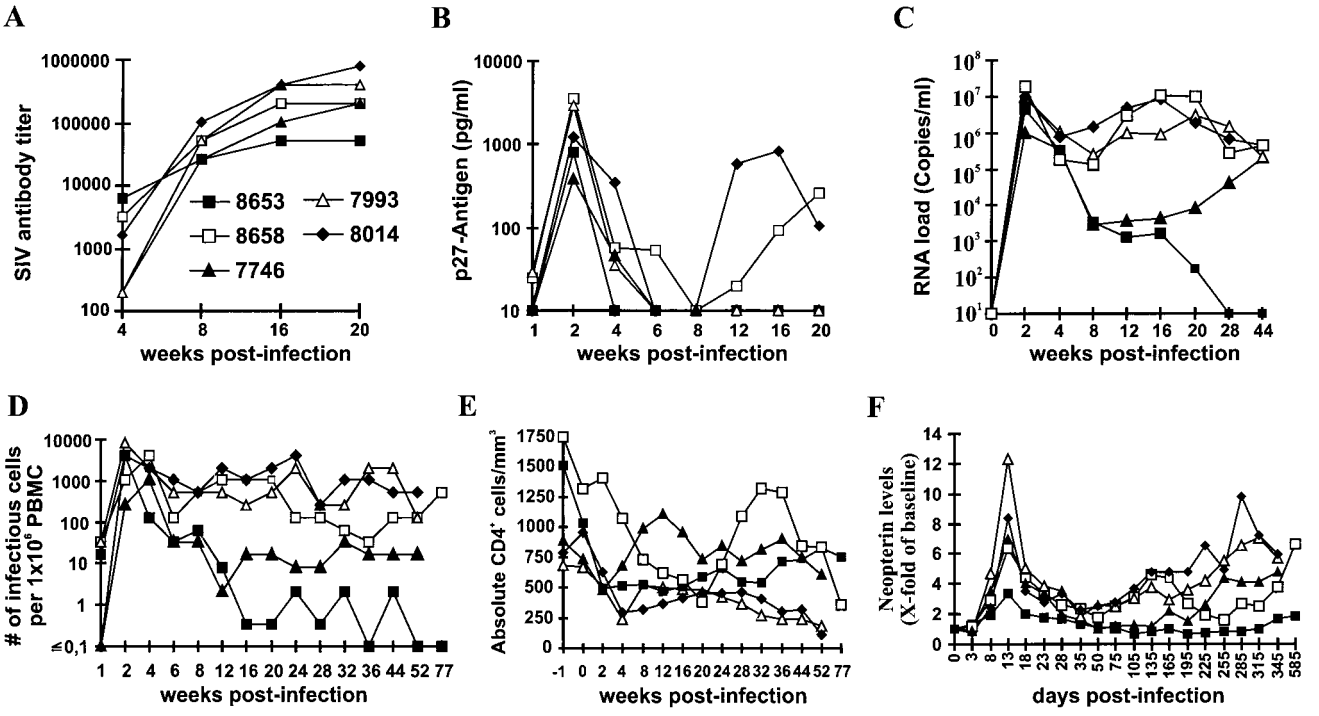

FIG. 10. In vitro properties of SHIV-40K6. Five macaques were infected with virus stocks containing 5 ng of p27 produced by COS-7 cells transfected with the SHIV-40K6 proviral construct. Panels: A, SIV enzyme-linked immunosorbent assay antibody titers; B, levels of p27 viremia; C, viral RNA load; D, cell-associated viral load; E, absolute CD4$^+$ T-cell count; F, urinary neopterin levels in infected animals. Parameters were determined as described in Materials and Methods. The neopterin/creatine ratio is expressed for each animal as the fold increase over the mean ratios determined prior to infection. Shown are mean values of at least three samples.

depletion and immunodeficiency in rhesus macaques. However, the clinical course of infection of rhesus macaques inoculated with Nef-SHIVs varied. Most of the animals showed characteristics of infection similar to those of pathogenic *nef*-open SIV infection. One of five macaques infected with Nef-SHIV40K6, however, showed low viral loads after the acute phase and remained asymptomatic, similar to animals infected with a virus with *nef* deleted. Host factors, and not the replicative capacity of the virus, seem to be a major determinant of the different outcome of Nef-SHIV infection, since these different patterns were observed after inoculation with the same dose of a molecular Nef-SHIV clone. All SHIV-infected macaques developed an efficient humoral immune response, and it remains to be elucidated why some animals could efficiently control these chimeras.

Reversions in premature stop codons in *nef* are selected to predominate within the first 2 weeks after infection (36). After coinfection of macaques with pathogenic SIV and an approximately 3,000-fold excess of a *nef* deletion mutant, the *nef*-open form came to predominate within a similar time frame (47). These previous findings show that an intact *nef* gene already provides a strong selective advantage very early in SIV infection. Therefore, it was unexpected that in macaques inoculated with the SHIVnef-Mix stock, forms containing HIV-1 *nef* alleles only came to predominate at 2 to 4 wpi (Fig. 3A). In the absence of an intact *nef* gene, SIV variants containing large deletions have a replicative advantage in vivo (38). Our results suggest that the levels of functionally active HIV-1 Nef expressed by the chimeric constructs used in the initial experiment were insufficient to stimulate SIV replication during the acute phase of infection. Perhaps the selective advantage of forms expressing even low levels of Nef is greater after the onset of the cellular immune response.

In the first animal passage, chimeras were selected that contained intact HIV-1 *nef* reading frames, as well as upstream nucleotide substitutions that enhanced Nef expression. Cloned chimeric viruses containing *env-nef*-LTR sequences derived from a slowly progressing Nef-SHIV-infected macaque replicated with almost SIVmac239 *nef*-open efficiency during the early stages of infection and were clearly more pathogenic than the initial virus stock. Thus, the nucleotide substitutions selected in vivo supported Nef-SHIV replication to higher titers. The high viral load observed in most animals inoculated with the second generation of Nef-SHIVs suggests that SIV Nef and HIV Nef exert similar effects in vivo. However, some sequence variations evolved that are rarely observed in *nef* alleles derived from HIV-1-infected humans, suggesting that the Nef proteins that are optimal for viral replication in simians and humans are slightly different. The N terminus of HIV-1 Nef is usually MGGKWS, whereas in SIVmac239 Nef it is MGGAIS. Thus, the W5L substitution, predicted by a number of *nef* alleles derived from Nef-SHIV infected macaques (Fig. 4), represents a change to an amino acid that is homologous to that usually found in SIV-Nef. Substitution of G3A, which was also frequently observed, is rarely found in both HIV-1 and SIV Nef. However, an alanine at position 3 is present in the majority of Nef sequences derived from HIV-2, which is highly related to SIVmac (53). A cysteine at position 59 was changed to valine in most Nef sequences obtained during later stages of Nef-SHIV infection. This cysteine residue is highly conserved among HIV-1 isolates (41, 65) and may be involved in formation of disulfide bonds (73). Nonetheless, *nef* alleles predicting

mutation of C59 were able to enhance viral replication and also active in MHC class I and CD4 downmodulation. Notably, these changes were not present in all of the *nef* alleles derived from progressing macaques and additional experiments on the functional relevance of these amino acid variations in Nef are needed to understand why they may be advantageous for SIV replication in macaques.

The two major goals of our study were (i) to investigate whether HIV-1 *nef* can functionally replace SIV *nef* in vivo and (ii) to establish a pathogenic Nef-SHIV model for the study of specific HIV-1 *nef* mutants and the evaluation of new therapeutic agents. The first goal has been almost fully achieved. However, infection of macaques with Nef-SHIVs as a model for the study of the role of HIV-1 Nef in disease induction has some limitations. Ideally, (i) the Nef-SHIVs should consistently replicate with high efficiency and induce disease within a year after infection, (ii) the Nef-SHIVs should be present as well-characterized molecular clones that allow the convenient analysis of *nef*, and (iii) the deduced protein sequences should contain all of the typical HIV-1 Nef features. The molecular SHIV-40K6 clone contains unique *Sst*II and *Mlu*I restriction sites flanking the *nef* gene, allowing convenient mutational analysis. As discussed above, some sequence variations in 40K6 Nef may reflect adaptation to the simian host. Nonetheless, the similarity of SHIV-40K6 Nef to the consensus Nef sequence derived from HIV-1-infected individuals is high and most typical HIV-1 Nef features were well conserved. However, although this molecular clone replicated efficiently early in infection, the $CD4^+$ lymphocyte counts remained stable in two of five infected macaques and one of these two animals was still asymptomatic with a low viral load after 80 weeks of follow-up. Thus, to study the impact of specific mutations in the HIV-1 *nef* gene on viral pathogenicity, one would have to inoculate a relatively high number of animals.

It may not be an easy task to generate Nef-SHIVs that reproducibly induce disease in all infected macaques. The SHIV-40K6 *nef* allele was active in altering T-cell receptor signaling and in downregulation of class I MHC and CD4. Furthermore, this HIV-1 *nef* allele was able to enhance SIV infectivity in sMAGI cells and replication in PBMC. This finding is similar to the results of Sinclair et al. (66). In contrast to the first in vivo passage, no consistent nucleotide substitutions in or upstream of the HIV-1 *nef* gene were observed in animals that progressed to immunodeficiency after infection with the SHIV-40K6 clone. Accordingly, the 40K6 *nef* allele might be almost optimal for replication in macaques and additional animal passages may not further enhance the pathogenicity of these chimeras. The effect of Nef on cell surface expression of CD4 and MHC class I depends strongly on Nef expression levels. Likely, reduced Nef expression by the chimeric constructs resulted in less efficient removal of CD4 and MHC class I from the infected-cell surface. Higher susceptibility of Nef-SHIV-infected cells to the antiviral immune response, compared to 239wt-infected cells, might explain why some chronically infected animals could efficiently control the chimeras. However, recent studies also suggest that HIV-1 and SIV Nef proteins interact in different ways with cellular proteins that are required for Nef-mediated downregulation of CD4 and class I MHC cell surface expression (13, 23, 24, 48) or are involved in signal transduction (43, 58). It remains to be elucidated if reduced HIV-1 Nef expression levels or functional differences between the two proteins are the major reason why HIV-1 Nef could not fully substitute for SIV Nef function in vivo.

In conclusion, we show that HIV-1 Nef expression enhances viral replication in rhesus macaques, indicating that they exert similar functions in vivo. Infection of macaques with a mixture of cloned chimeric viruses might allow the evaluation of therapeutic agents that block HIV-1 Nef function. During the acute phase of infection, the SHIV-40K6 clone generated in this study replicated with much higher efficiency in rhesus macaques than did SIV with *nef* deleted. Thus, this chimera can be used to test the impact of specific mutations in HIV-1 *nef* on viral replication in vivo. However, it failed to induce disease in some infected animals. Therefore, the development of Nef-SHIVs that consistently induce simian AIDS within a reasonably short time frame would clearly increase the value of this animal model for the analysis of specific HIV-1 Nef functions.

ACKNOWLEDGMENTS

We thank Mandy Krumbiegel and Marion Hamacher for excellent technical assistance and Bernhard Fleckenstein for constant support and encouragement. We also thank Ronald C. Desrosiers for providing 221 and CEMx174-SEAP cells and for helpful discussions. We are also indebted to Julie Overbaugh and Bryce Chackerian for providing sMAGI cells.

This work was supported by BMBF grant 01Ki9478, the Deutsche Forschungsgemeinschaft (SFB466), the Sander Stiftung, and PHS grant IA42561 (to J.S.).

ADDENDUM IN PROOF

After submission of the manuscript, similar findings were reported by Alexander et al. (L. Alexander, Z. Du, A. Y. M. Howe, S. Czajak, and R. C. Desrosiers, J. Virol. **73:**5814–5825, 1999).

REFERENCES

1. **Aiken, C., J. Konner, N. R. Landau, M. E. Lenburg, and D. Trono.** 1994. Nef induces CD4 endocytosis: requirement for a critical dileucine motif in the membrane-proximal CD4 cytoplasmic domain. Cell **76:**853–864.
2. **Alexander, L., Z. Du, M. Rosenzweig, J. V. Jung, and R. C. Desrosiers.** 1997. A role for natural simian immunodeficiency virus and human immunodeficiency virus type 1 Nef alleles in lymphocyte activation. J. Virol. **71:**6094–6099.
3. **Anderson, S., D. C. Shugars, R. Swanstrom, and J. V. Garcia.** 1993. Nef from primary isolates of human immunodeficiency virus type 1 suppresses surface CD4 expression in human and mouse T cells. J. Virol. **67:**4923–4931.
4. **Arold, S., P. Franken, M. P. Strub, F. Hoh, S. Benichou, R. Benarous, and C. Dumas.** 1997. The crystal structure of HIV-1 Nef protein bound to the Fyn kinase SH3 domain suggests a role for this complex in altered T cell receptor signaling. Structure **5:**1361–1372.
5. **Baur, A. S., E. T. Sawai, P. Dazin, W. J. Fantl, C. Cheng-Mayer, and B. M. Peterlin.** 1994. HIV-1 Nef leads to inhibition or activation of T cells depending on its intracellular localization. Immunity **1:**373–384.
6. **Bell, J., J. Maughan, E. Hooker, F. Cook, and T. A. Reinhart.** 1998. Association of simian immunodeficiency virus Nef with the T-cell receptor (TCR) ζ chain leads to TCR downmodulation. J. Gen. Virol. **79:**2717–2727.
7. **Benson, R. E., A. Sanfridson, J. S. Ottinger, C. Doyle, and B. R. Cullen.** 1993. Downregulation of cell-surface CD4 expression by simian immunodeficiency virus Nef prevents viral super-infection. J. Exp. Med. **177:**1561–1566.
8. **Bresnahan, P. A., W. Yonemoto, S. Ferell, D. Williams-Herman, R. Geleziumas, and W. C. Greene.** 1998. A dileucine motif in HIV-1 Nef acts as an internalization signal for CD4 downregulation and binds the AP-1 clathrin adaptor. Curr. Biol. **22:**1235–1238.
9. **Chackerian, B., N. L. Haigwood, and J. Overbaugh.** 1995. Characterization of a CD4-expressing macaque cell line that can detect virus after a single replication cycle and can be infected by diverse simian immunodeficiency virus isolates. Virology **213:**386–394.
10. **Chowers, M. Y., C. A. Spina, T. J. Kwoh, N. J. S. Fitch, D. D. Richman, and J. C. Guatelli.** 1994. Optimal infectivity in vitro of human immunodeficiency virus type 1 requires an intact *nef* gene. J. Virol. **68:**2906–2914.
11. **Collette, Y., H. Dutartre, A. Benziane, A. Ramos-Morales, R. Benarous, M. Harris, and D. Olive.** 1996. Physical and functional interaction of Nef with Lck. HIV-1 Nef-induced T-cell signaling defects. J. Biol. Chem. **271:**6333–6341.
12. **Collins, K. L., B. K. Chen, S. A. Kalams, B. D. Walker, and D. Baltimore.** 1998. HIV-1 Nef protein protects infected primary cells against killing by cytotoxic T lymphocytes. Nature **391:**397–401.
13. **Craig, H. M., M. W. Pandori, and J. C. Guatelli.** 1998. Interaction of HIV-1 Nef with cellular dileucine-based sorting pathway is required for CD4 down-

regulation and optimal viral infectivity. Proc. Natl. Acad. Sci. USA **95:**11229–11234.
14. **Cullen, B. R.** 1987. Use of eukaryotic expression technology in the functional analysis of cloned genes. Methods Enzymol. **152:**684–703.
15. **De, S. K., and J. W. Marsh.** 1994. HIV-1 Nef inhibits a common activation pathway in NIH-3T3 cells. J. Biol. Chem. **269:**6656–6660.
16. **Deacon, N. J., A. Tsykin, A. Solomon, K. Smith, M. Ludford-Menting, D. J. Hooker, D. A. McPhee, A. L. Greenway, A. Ellett, and C. Chatfield.** 1995. Genomic structure of an attenuated quasi species of HIV-1 from a blood transfusion donor and recipients. Science **270:**988–991.
17. **Deng, H., R. Liu, W. Ellmeier, S. Choe, D. Unutmaz, M. Burkhart, P. Di Marzio, S. Marmon, R. E. Sutton, C. M. Hill, C. B. Davis, S. C. Peiper, T. J. Schall, D. R. Littman, and N. R. Landau.** 1996. Identification of a major co-receptor for primary isolates of HIV-1. Nature **381:**661–666.
18. **deRonde, A., B. Klaver, W. Keulen, L. Smit, and J. Goudsmit.** 1992. Natural HIV-1 NEF accelerates virus replication in primary human lymphocytes. Virology **188:**391–395.
19. **Du, Z., S. M. Lang, V. G. Sasseville, A. A. Lackner, P. O. Ilyinskii, M. D. Daniel, J. U. Jung, and R. C. Desrosiers.** 1995. Identification of a *nef* allele that causes lymphocyte activation and acute disease in macaque monkeys. Cell **82:**665–674.
20. **Fendrich, C., W. Lüke, C. Stahl-Hennig, O. Herchenröder, D. Fuchs, H. Wachter, and G. Hunsmann.** 1989. Urinary neopterin concentrations in rhesus monkeys after infection with simian immunodeficiency virus (SIVmac251). AIDS **3:**305–307.
21. **Garcia, J. V., and A. D. Miller.** 1991. Serine phosphorylation-independent downregulation of cell-surface CD4 by nef. Nature **350:**508–511.
22. **Goldsmith, M. A., M. T. Warmerdam, R. E. Atchison, M. D. Miller, and W. C. Greene.** 1995. Dissociation of the CD4 downregulation and viral infectivity enhancement functions of human immunodeficiency virus type 1 Nef. J. Virol. **69:**4112–4121.
23. **Greenberg, M., L. DeTulleo, I. Rapoport, J. Skowronski, and T. Kirchhausen.** 1998. A dileucine motif in HIV-1 Nef is essential for sorting into clathrin-coated pits and for downregulation of CD4. Curr. Biol. **22:**1239–1242.
24. **Greenberg, M. E., A. J. Iafrate, and J. Skowronski.** 1998. The SH3 domain-binding surface and an acidic motif in HIV-1 Nef regulate trafficking of class I MHC complexes. EMBO J. **17:**2777–2789.
25. **Greenway, A., A. Azad, and D. McPhee.** 1995. Human immunodeficiency virus type 1 Nef protein inhibits activation pathways in peripheral blood mononuclear cells and T-cell lines. J. Virol. **69:**1842–1850.
26. **Gundlach, B. R., H. Linhart, U. Dittmer, S. Sopper, S. Reiprich, D. Fuchs, B. Fleckenstein, G. Hunsmann, C. Stahl-Hennig, and K. Überla.** 1997. Construction, replication, and immunogenic properties of a simian immunodeficiency virus expressing interleukin-2. J. Virol. **71:**2225–2232.
27. **Guy, B., M. P. Kieny, Y. Riviere, C. Le Peuch, K. Dott, M. Girard, L. Montagnier, and J. P. Lecocq.** 1987. HIV F/3′ orf encodes a phosphorylated GTP-binding protein resembling an oncogene product. Nature **330:**266–269.
28. **Higgins, J. R., S. Sutjipto, P. A. Marx, and N. C. Pedersen.** 1992. Shared antigenic epitopes of the major core proteins of human and simian immunodeficiency virus isolates. J. Med. Primatol. **21:**265–269.
29. **Ho, S. N., H. D. Hunt, R. M. Horton, J. K. Pullen, and L. R. Pease.** 1989. Site directed mutagenesis by overlap extension using the polymerase chain reaction. Gene **77:**51–59.
30. **Howe, A. Y. M., J. U. Jung, and R. C. Desrosiers.** 1998. Zeta chain of the T-cell receptor interacts with Nef of simian immunodeficiency virus and human immunodeficiency virus type 2. J. Virol. **72:**9827–9834.
31. **Hua, J., and B. R. Cullen.** 1997. Human immunodeficiency virus types 1 and 2 and simian immunodeficiency virus Nef use distinct but overlapping target sites for downregulation of cell surface CD4. J. Virol. **71:**6742–6748.
32. **Huang, Y., L. Zhang, and D. D. Ho.** 1995. Characterization of *nef* sequences in long-term survivors of human immunodeficiency virus type 1 infection. J. Virol. **69:**93–100.
33. **Iafrate, A. J., S. Bronson, and J. Skowronski.** 1997. Separable functions of Nef disrupt two aspects of T cell receptor machinery: CD4 expression and CD3 signaling. EMBO J. **16:**673–684.
34. **Karlsson, G. B., M. Halloran, J. Li, I.-W. Park, R. Gomila, K. A. Reimann, M. K. Axthelm, S. A. Iliff, N. L. Letvin, and J. Sodroski.** 1997. Characterization of molecularly cloned simian-human immunodeficiency viruses causing rapid $CD4^+$ lymphocyte depletion in rhesus monkeys. J. Virol. **71:**4218–4225.
35. **Kestler, H. W., T. Kodama, D. J. Ringler, M. Marthas, N. Pedersen, A. Lackner, D. Regier, P. K. Sehgal, M. D. Daniel, and R. C. Desrosiers.** 1990. Induction of AIDS in rhesus monkeys by molecularly cloned simian immunodeficiency virus. Science **248:**1109–1112.
36. **Kestler, H. W., D. J. Ringler, K. Mori, D. L. Panicali, P. K. Sehgal, M. D. Daniel, and R. C. Desrosiers.** 1991. Importance of the *nef* gene for maintenance of high virus loads and for development of AIDS. Cell **65:**651–662.
37. **Khan, I. H., E. T. Sawai, E. Antonio, C. J. Weber, C. P. Mandell, P. Montbriand, and P. A. Luciw.** 1998. Role of the SH3-ligand domain of simian immunodeficiency virus Nef in interaction with Nef-associated kinase and simian AIDS in rhesus macaques. J. Virol. **72:**5820–5830.
38. **Kirchhoff, F., H. W. Kestler III, and R. C. Desrosiers.** 1994. Upstream U3 sequences in simian immunodeficiency virus are selectively deleted in vivo in the absence of an intact *nef* gene. J. Virol. **68:**2031–2037.
39. **Kirchhoff, F., T. C. Greenough, D. B. Brettler, J. L. Sullivan, and R. C. Desrosiers.** 1995. Absence of intact nef sequences in a long-term, nonprogressing survivor of HIV-1 infection. N. Engl. J. Med. **332:**228–232.
40. **Kirchhoff, F., S. Pöhlmann, M. Hamacher, R. E. Means, T. Kraus, K. Überla, and P. Di Marzio.** 1997. Simian immunodeficiency virus variants with differential T-cell and macrophage tropism use CCR5 and an unidentified cofactor expressed in CEMx174 cells for efficient entry. J. Virol. **71:**6509–6516.
41. **Kirchhoff, F., P. J. Easterbrook, N. Douglas, M. Troop, T. C. Greenough, J. Weber, S. Carl, J. L. Sullivan, and R. S. Daniels.** 1999. Sequence variations in human immunodeficiency virus type 1 Nef are associated with a different stages of disease. J. Virol. **73:**5497–5508.
42. **Kozak, M.** 1986. Point mutations define a sequence flanking the AUG initiator codon that modulates translation by eukaryotic ribosomes. Cell **44:**283–292.
43. **Lang, S. M., A. J. Iafrate, C. Stahl-Hennig, E. M. Kuhn, T. Nißlein, M. Haupt, G. Hunsmann, J. Skowronski, and F. Kirchhoff.** 1997. Association of simian immunodeficiency virus Nef with cellular serine/threonine kinases is dispensable for the development of AIDS in rhesus macaques. Nat. Med. **3:**860–865.
44. **Lee, C. H., B. Leung, M. A. Lemmon, J. Zheng, D. Cowburn, J. Kuriyan, and K. Saksela.** 1995. A single amino acid in the SH3 domain of Hck determines its high affinity and specificity in binding to HIV-1 Nef protein. EMBO J. **14:**5006–5015.
45. **Lee, C. H., K. Saksela, U. A. Mirza, B. T. Chait, and J. Kuriyan.** 1996. Crystal structure of the conserved core of HIV-1 Nef complexed with a Src family SH3 domain. Cell **85:**931–942.
46. **Le Gall, S., M. C. Prevost, J. M. Heard, and O. Schwartz.** 1997. Human immunodeficiency virus type 1 Nef independently affects virion incorporation of major histocompatibility complex class I molecules and virus infectivity. Virology **229:**295–301.
47. **Linhart, H., B. R. Gundlach, S. Sopper, U. Dittmer, K. Matz-Rensing, E. M. Kuhn, J. Muller, G. Hunsmann, C. Stahl-Hennig, and K. Uberla.** 1997. Live attenuated SIV vaccines are not effective in a postexposure vaccination model. AIDS Res. Hum. Retroviruses **13:**593–599.
48. **Lock, M., M. E. Greenberg, A. J. Iafrate, T. Swigut, J. Münch, F. Kirchhoff, N. Shohdy, and J. Skowronski.** 1999. Two elements target SIV Nef to the AP-2 clathrin adaptor complex, but only one is required for the induction of CD4 endocytosis. EMBO J. **18:**2722–2733.
49. **Luria, S., I. Chambers, and P. Berg.** 1991. Expression of the type 1 human immunodeficiency virus Nef protein in T cells prevents antigen receptor-mediated induction of interleukin 2 mRNA. Proc. Natl. Acad. Sci. USA **88:**5326–5330.
50. **Mariani, R., and J. Skowronski.** 1993. CD4 down-regulation by nef alleles isolated from human immunodeficiency virus type 1-infected individuals. Proc. Natl. Acad. Sci. USA **90:**5549–5553.
51. **Michael, N. L., G. Chang, L. A. d'Arcy, C. J. Tseng, D. L. Birx, and H. W. Sheppard.** 1995. Functional characterization of human immunodeficiency virus type 1 *nef* genes in patients with divergent rates of disease progression. J. Virol. **69:**6758–6769.
52. **Miller, M. D., M. T. Warmerdam, I. Gaston, W. C. Greene, and M. B. Feinberg.** 1994. The human immunodeficiency virus-1 *nef* gene product: a positive factor for viral infection and replication in primary lymphocytes and macrophages. J. Exp. Med. **179:**101–114.
53. **Myers, G., B. Korber, S. Wain-Hobson, and R. F. Smith.** 1993. Human retroviruses and AIDS. Los Alamos National Laboratory, Los Alamos, N. Mex.
54. **Nunn, M. F., and J. W. Marsh.** 1996. Human immunodeficiency virus type 1 Nef associates with a member of the p21-activated kinase family. J. Virol. **70:**6157–6161.
55. **Piguet, V., Y. L. Chen, A. Mangasarian, M. Foti, J. L. Carpentier, and D. Trono.** 1998. Mechanism of Nef-induced CD4 endocytosis: Nef connects CD4 with the mu chain of adaptor complexes. EMBO J. **17:**2472–2481.
56. **Potts, B. J.** 1990. "Mini" reverse transcriptase (RT) assay, p. 103–106. *In* A. Aldovini, and B. D. Walker (ed.), Techniques in HIV research. Stockton, New York, N.Y.
57. **Regier, D. A., and R. C. Desrosiers.** 1989. The complete nucleotide sequence of a pathogenic molecular clone of SIV. AIDS Res. Hum. Retroviruses **6:**1221–1231.
58. **Saksela, K., G. Cheng, and D. Baltimore.** 1995. Proline-rich (PxxP) motifs in HIV-1 Nef bind to SH3 domains of a subset of Src kinases and are required for the enhanced growth of Nef^+ viruses but not for down-regulation of CD4. EMBO J. **14:**484–491.
59. **Salvi, R., A. R. Garbuglia, A. Di Caro, S. Pulciani, F. Montella, and A. Benedetto.** 1998. Grossly defective *nef* gene sequences in a human immunodeficiency virus type 1-seropositive long-term nonprogressor. J. Virol. **72:**3646–3657.
60. **Sanfridson, A., B. R. Cullen, and C. Doyle.** 1994. The simian immunodefi-

ciency virus Nef protein promotes degradation of CD4 in human T cells. J. Biol. Chem. **269:**3917–3920.
61. **Sawai, E. T., A. Baur, H. Struble, B. M. Peterlin, J. A. Levy, and C. Cheng-Mayer.** 1994. Human immunodeficiency virus type 1 Nef associates with a cellular serine kinase in T lymphocytes. Proc. Natl. Acad. Sci. USA **91:**1539–1543.
62. **Schwartz, O., V. Marechal, S. Le Gall, F. Lemonnier, and J. M. Heard.** 1996. Endocytosis of major histocompatibility complex class I molecules is induced by the HIV-1 Nef protein. Nat. Med. **2:**338342.
63. **Shibata, R., M. Kawamura, H. Sakai, M. Hayami, A. Ishimoto, and A. Adachi.** 1991. Generation of a chimeric human and simian immunodeficiency virus infectious to monkey peripheral blood mononuclear cells. J. Virol. **65:**3514–3520.
64. **Shibata, R., F. Maldarelli, C. Siemon, T. Matano, M. Parta, G. Miller, T. Fredrickson, and M. A. Martin.** 1997. Infection and pathogenicity of chimeric simian-human immunodeficiency viruses in macaques: determinants of high virus loads and CD4 cell killing. J. Infect. Dis. **176:**362–373.
65. **Shugars, D. C., M. S. Smith, D. H. Glueck, P. V. Nantermet, F. Seillier-Moiseiwitsch, and R. Swanstrom.** 1993. Analysis of human immunodeficiency virus type 1 *nef* gene sequences present in vivo. J. Virol. **67:**4639–4650.
66. **Sinclair, E., P. Barbosa, and M. B. Feinberg.** 1997. The *nef* gene products of both simian and human immunodeficiency viruses enhance virus infectivity and are functionally interchangeable. J. Virol. **71:**3641–3651.
67. **Skowronski, J., D. Parks, and R. Mariani.** 1993. Altered T cell activation and development in transgenic mice expressing the HIV-1 *nef* gene. EMBO J. **12:**703–713.
68. **Skowronski, J., and R. Mariani.** 1995. Transient assay for Nef-induced down-regulation of CD4 antigen expression on the cell surface, p. 231–242. *In* J. Karn (ed.), HIV-1: a practical approach. Oxford University Press, Oxford, England.
69. **Spina, C. A., T. J. Kwoh, M. Y. Chowers, J. C. Guatelli, and D. D. Richman.** 1994. The importance of nef in the induction of human immunodeficiency virus type 1 replication from primary quiescent CD4 lymphocytes. J. Exp. Med. **179:**115–123.
70. **Stahl-Hennig, C., O. Herchenröder, S. Nick, M. Evers, M. Stille-Siegener, K.-D., Jentsch, F., Kirchhoff, T., Tolle, T. J. Gatesmann, W. Lüke, and G. Hunsmann.** 1990. Experimental infection of macaques with HIV-2BEN a novel HIV-2 isolate. AIDS **4:**611–617.
71. **Stahl-Hennig, C., G. Voss, S. Nick, H. Petry, D. Fuchs, H. Wachter, C. Coulibaly, W. Lüke, and G. Hunsmann.** 1992. Immunization with Tween-ether-treated SIV adsorbed onto aluminum hydroxide protects monkeys against experimental SIV infection. Virology **186:**588–596.
72. **Ten Haaft, P., B. Verstrepen, K. Überla, B. Rosenwirth, and J. Heeney.** 1998. A pathogenic threshold of virus load defined in simian immunodeficiency virus- or simian-human immunodeficiency virus-infected macaques. J. Virol. **72:**10281–10285.
73. **Zazopoulos, E., and W. A. Haseltine.** 1993. Effect of *nef* alleles on replication of human immunodeficiency virus type 1. Virology **194:**20–27.